MCB
Journals.ASM.org

# PERK Is Required in the Adult Pancreas and Is Essential for Maintenance of Glucose Homeostasis

Yan Gao,[a,b] Daniel J. Sartori,[d] Changhong Li,[d] Qian-Chun Yu,[c] Jake A. Kushner,[d,e] M. Celeste Simon,[a,b,c,f] and J. Alan Diehl[a,b,c]

The Abramson Family Cancer Research Institute,[a] Department of Cancer Biology,[b] Abramson Cancer Center and Perelman School of Medicine,[c] Division of Endocrinology and Diabetes, Children's Hospital of Philadelphia,[d] and Howard Hughes Medical Institute,[f] University of Pennsylvania, Philadelphia, Pennsylvania, USA, and Pediatric Diabetes and Endocrinology, Baylor College of Medicine, and Texas Children's Diabetes and Endocrine Care Center, Texas Children's Hospital, Houston, Texas, USA[e]

**Germ line PERK mutations are associated with diabetes mellitus and growth retardation in both rodents and humans. In contrast, late embryonic excision of PERK permits islet development and was found to prevent onset of diabetes, suggesting that PERK may be dispensable in the adult pancreas. To definitively establish the functional role of PERK in adult pancreata, we generated mice harboring a conditional PERK allele in which excision is regulated by tamoxifen administration. Deletion of PERK in either young adult or mature adult mice resulted in hyperglycemia associated with loss of islet and β cell architecture. PERK excision triggered intracellular accumulation of proinsulin and Glut2, massive endoplasmic reticulum (ER) expansion, and compensatory activation of the remaining unfolded-protein response (UPR) signaling pathways specifically in pancreatic tissue. Although PERK excision increased β cell death, this was not a result of decreased proliferation as previously reported. In contrast, a significant and specific increase in β cell proliferation was observed, a result reflecting increased cyclin D1 accumulation. This work demonstrates that contrary to expectations, PERK is required for secretory homeostasis and β cell survival in adult mice.**

The endoplasmic reticulum (ER) serves as a primary coordinator of secretory protein maturation. Protein trafficking and folding within the ER are under the surveillance of a signal transduction pathway referred to as the unfolded-protein response (UPR). The UPR pathway consists of three distinct signaling molecules, PKR-like kinase (PERK), inositol-requiring enzyme 1 (Ire1α/β), and the transmembrane transcription factor ATF6 (9); signaling via these factors serves to adaptively adjust the functional capacity of the ER. Any perturbation of this check-and-balance mechanism will lead to misfolded-protein accumulation in the ER and further affect cellular homeostasis.

Pancreatic β cells are specialized cells that synthesize and secrete insulin to control blood glucose levels. The precursor of insulin, preproinsulin, is synthesized on the ribosomes of the rough ER with a signal peptide, which is cleaved to generate proinsulin in the ER. In the lumen of the ER, proinsulin is properly folded and then transported to the Golgi apparatus for packaging and secretion. The conversion of proinsulin to insulin takes place in the secretory granules, and subsequently, mature insulin is released by exocytosis (15). Physiologically, the amounts of insulin biogenesis and secretion are partially determined by blood glucose fluctuations and by PERK-dependent phosphorylation of eukaryotic translation initiation factor 2 (eIF2α), which, in turn, helps adjust the amount of protein delivered into the ER lumen (8, 36). In the absence of eIF2α phosphorylation, which has been achieved via the generation of mice harboring a homozygous knock-in of eIF2αSer51/Ala, mice developed a severe diabetic phenotype (36), demonstrating a requisite role for translational control during β cell development.

PERK expression is high in the mouse pancreas, and analogous with findings in eIF2αSer51/Ala knock-in mice, PERK deficiency during embryogenesis triggers permanent neonatal diabetes mellitus with exocrine pancreatic atrophy and reduced insulin secretion (18, 42). The conventional PERK knockout phenotype is also remarkably similar to that observed in individuals afflicted with Wolcott-Rallison syndrome (WRS), a recessive disorder characterized by a loss-of-function PERK mutation (19, 37, 42, 43). Surprisingly, additional work with mice in which PERK excision is developmentally regulated suggests that embryonic day 14 through postnatal day 4 is in fact the only critical period for PERK function; beyond this point, PERK function was not required (43). However, whether PERK activity is required for adult glucose homeostasis and the nature of the relationship between PERK and β cell proliferation remain controversial.

Given recent work suggesting that the development of small-molecule inhibitors of PERK may have significant utility in the treatment of a variety of neoplastic diseases (2, 4), we set out to definitively assess the importance of PERK in adult mice through generation of an acutely inducible PERK knockout model. PERK ablation in adult mice triggered β cell death, which was preceded by the aberrant accumulation of immature insulin, activation of the remaining UPR branches, and increased β cell proliferation. Physiologically, this was accompanied by a loss of glucose homeostasis and the onset of an acute diabetic phenotype. Thus, in contrast to previous studies, this work demonstrates that PERK function is essential for adult pancreatic homeostasis.

## MATERIALS AND METHODS

**Animal husbandry.** Cre-ERT2; PERK$^{l/l}$ ("l" indicates loxP) and Cre-ERT2; PERK$^{+/l}$ mice were generated by intercrossing PERK$^{l/l}$ or PERK$^{+/l}$ mice to Cre-ERT2 heterozygous mice. Cre-ERT2; PERKwt mice were generated by intercrossing Cre-ERT2; PERK$^{+/l}$ to PERK$^{+/l}$ mice or by mating

Received 25 July 2012 Returned for modification 17 August 2012
Accepted 6 October 2012
Published ahead of print 15 October 2012
Address correspondence to J. Alan Diehl, adiehl@mail.med.upenn.edu.
Supplemental material for this article may be found at http://mcb.asm.org/.

doi:10.1128/MCB.01009-12

wild-type mice to Cre-ERT2 mice. For PERK deletion, tamoxifen (TAM; Sigma) was administered once a day via oral gavage for 5 days at a dose of 0.20 mg/g of body weight/day. Time post-tamoxifen treatment was determined from end treatment. Pdx1-CreER; $PERK^{l/l}$ mice were generated by intercrossing Pdx1-CreER with $PERK^{l/l}$ mice. The genotypes were verified by PCR using tail, pancreas tissue, and islet DNA.

Blood glucose was measured using a Freestyle meter (TheraSense, Inc.). Insulin concentrations were determined by enzyme-linked immunosorbent assay (ELISA) using mouse insulin as a standard (Crystal Chem). Glucose tolerance tests (GTT; glucose at 2 g/kg of body weight by oral gavage) and insulin tolerance tests (ITT; insulin at 1 IU/kg of body weight, given intraperitoneally [i.p.]) were conducted. For insulin rescue, mice received a subcutaneous injection of phosphate-buffered saline (PBS) or insulin (5 IU/kg or 10 IU/kg; Novolin) for 4 weeks, and the whole pancreas was harvested for immunostaining analysis.

**Insulin secretion and cytosolic $Ca^{2+}$ measurements in isolated islets.** Islet isolation, perifusion, and cytosolic calcium ($[Ca^{2+}]_i$) measurement were described previously (27, 28). In brief, islets were isolated from 2 or 3 mice from each genotype by collagenase digestion and cultured with 10 mM glucose in RPMI 1640 medium (Sigma) for 3 to 4 days. Islets were perifused in a Krebs-Ringer bicarbonate buffer (KRBB) with 0.25% bovine serum albumin (BSA) at a flow rate of 1 ml/min. Insulin was measured by radioimmunoassay. $[Ca^{2+}]_i$ was measured by dual-wavelength fluorescence microscopy using a Zeiss AxioVision system.

**Immunohistochemistry, BrdU incorporation, and terminal deoxynucleotidyltransferase-mediated dUTP-biotin nick end labeling (TUNEL) assays.** Mice were sacrificed, and tissues were harvested and fixed in 4% paraformaldehyde for 12 to 16 h. Tissues were washed with PBS, dehydrated in gradient ethanol, and embedded in paraffin. Tissue sections (5 μm) were subjected to immunostaining using primary antibodies against the following: insulin (Invitrogen), proinsulin (Ole D. Madsen, Beta Cell Biology Consortium), Glut2 (Millipore), Glut4 (Abcam), bromodeoxyuridine (BrdU) (Rockland), and ApoE (Abcam). Paraffin-embedded tissue sections were incubated with anti-BrdU antibody. Secondary antibodies labeled with Cy2, Cy3, or Cy5 (Jackson ImmunoResearch Laboratories Inc.) were applied following the primary antibody incubation. Nuclear staining was performed with 4′6-diamidino-2-phenylindole (DAPI) (Promega).

Mice were labeled continuously with BrdU by substituting drinking water with bottles containing 1 mg/ml BrdU (Sigma) for 1 or 2 weeks. Immunostaining was performed, and photomicrograph images were captured with a Hamamatsu Orca ER digital camera.

TUNEL was performed using Cy5-labeled reagents (Roche) on rehydrated and trypsin-predigested pancreas sections. Sections were subsequently stained for insulin and appropriate secondary antibody according to the description above.

**qPCR.** Total RNA was extracted from purified mouse islets using TRIzol (Invitrogen) by following the manufacturer's instructions. cDNA was synthesized by using Moloney murine leukemia virus (MMLV) reverse transcriptase III and random primers (Invitrogen) according to the manufacturer's protocol. Quantitative real-time PCR (qPCR) assay was prepared by using Sybr PCR mix (Applied Biosystems) and amplification using the ABI Prism 7000 sequence detection system (Applied Biosystems) with the following primers: Bip (F), 5′-ACCCTTACTCGGGCCAAATT-3′; Bip (R), 5′-AGAGCGGAACAGGTCCATGT-3′; Grp94 (F), 5′-CTGGGTCAAGCAGAAAGGAG-3′; Grp94 (R), 5′-TCTCTGTTGCTTCCCGACTT-3′; EDEM (F), 5′-TTCCAGCCTTTGAAAACACC-3′; EDEM (R), 5′-TGCTGTCAGGAGGAACACCT-3′; CHOP (F), 5′-CCAACAGAGGTCACACGCAC-3′; CHOP (R), 5′-TGACTGGAATCTGGAGAGCGA-3′; Der1 (F), 5′-CACCAGCCATGCTAAGCAGA-3′; Der1 (R), 5′-TCAGTGTGGGTCAGGTCCAAG-3′; glyceraldehyde-3-phosphate dehydrogenase (GAPDH) (F), 5′-GGAGCGAGACCCCACTAACA-3′; and GAPDH (R), 5′-ACATACTCAGCACCGGCCTC-3′.

**Western analysis.** Islets purified from 3 to 5 mice of each genotype were lysed in Tween 20 buffer containing 50 mM HEPES (pH 8.0), 150 mM NaCl, 2.5 mM EGTA, 1 mM EDTA, 0.1% Tween 20, and protease and phosphatase inhibitors (1 mM phenylmethylsulfonyl fluoride, 20 U of aprotinin/ml, 5 mg of leupeptin/ml, 1 mM dithiothreitol [DTT], 0.4 mM NaF, and 10 mM β-glycerophosphate). Lysates were sonicated prior to clearing by centrifugation at 4°C for 30 min. Lysate protein concentration was determined by bicinchoninic acid (BCA) assay, and proteins were resolved by SDS-PAGE, transferred to nitrocellulose membranes, and subjected to immunoblotting. Antibodies utilized include antibodies against p-eIF2α (S51), Bip, eIF2α (Invitrogen), cyclin D1 mouse monoclonal D1-72-13G, ATF6 (Abcam), XBP1 (Santa Cruz), Cul4a (Bethyl), Ire1α (Cell Signaling), and β-actin (Sigma) and p-JNK antibodies from Cell Signaling Corp.

**Statistical analysis.** Data are presented as means ± standard errors of the means (SEM). For two-group comparison, a two-tailed Student *t* test was used; for multiple-group comparison, one-way analysis of variance (ANOVA) (Igor) was used. A *P* value of $<0.05$ was considered statistically significant.

## RESULTS

**Generation of acute PERK knockout mice.** To generate mice in which PERK could be inducibly excised, we intercrossed mice with a Ubc9 promoter-driven Cre-ERT2 transgene with mice harboring a floxed allele of PERK ($PERK^{l/l}$), thereby generating a Cre-ERT2; $PERK^{l/l}$ genotype. Tamoxifen was administered at 8 to 12 weeks (young adult) or 6 months (aging cohort) to generate the following genotypes: PERK knockout ($PERK^{\Delta/\Delta}$); PERK heterozygous ($PERK^{+/\Delta}$); PERK wild type (WT), including Cre-ERT2; PERKwt (without loxP sites); and $PERK^{l/l}$ (loxP sites, no Cre-ERT2) (Fig. 1A) (34, 42). PERK excision efficiency was estimated to be 60 to 70% (see Fig. S1A in the supplemental material). Significantly, PERK protein levels were undetectable in pancreata from $PERK^{\Delta/\Delta}$ mice (Fig. 1B). $PERK^{\Delta/\Delta}$ mice exhibited mildly reduced growth when excised at 8 weeks of age (Fig. 1C, photos I and II), while $PERK^{+/\Delta}$ mice were negligibly smaller than wild-type mice (data not shown). Strikingly, there was no body size difference between the various genotypes when PERK excision was performed in mice at 6 months of age (Fig. 1C, photos III and IV).

**Acute PERK excision triggers diabetes mellitus.** To address any requirements for PERK in the maintenance of glucose homeostasis in adult mice, 8-week-old and 6-month-old Cre-ERT2; $PERK^{l/l}$ and control mice were treated with TAM and maintained on a normal chow diet; blood glucose levels were subsequently monitored at regular intervals (Fig. 1D and 2A). Regardless of the age of excision, $PERK^{\Delta/\Delta}$ mice exhibited moderate hyperglycemia (~200 mg/dl) by 1 month postexcision and progressively developed severe hyperglycemia (>500 to 600 mg/dl) within 2 months. Glucose tolerance tests (GTT) revealed an inability of $PERK^{\Delta/\Delta}$ mice to regulate glucose levels (Fig. 1E); knockout mice also exhibited decreased insulin secretion in response to glucose challenge (Fig. 1F). Critically, we noted that $PERK^{+/\Delta}$ mice were euglycemic at fed status and responded normally in GTT (Fig. 1E), although insulin secretion was decreased compared to that in PERK wild-type (WT) mice following challenge (Fig. 1F). We also noted that the plasma insulin levels in PERK-deficient mice were significantly reduced relative to those in age-matched controls, while no significant difference between $PERK^{+/\Delta}$ and wild-type mice was noted (see Fig. S1B in the supplemental material). Moreover, insulin tolerance tests (ITT) revealed that acute PERK excision did not abolish insulin sensitivity in peripheral tissues (see Fig. S1C), suggesting this diabetic phenotype reflects a lack of

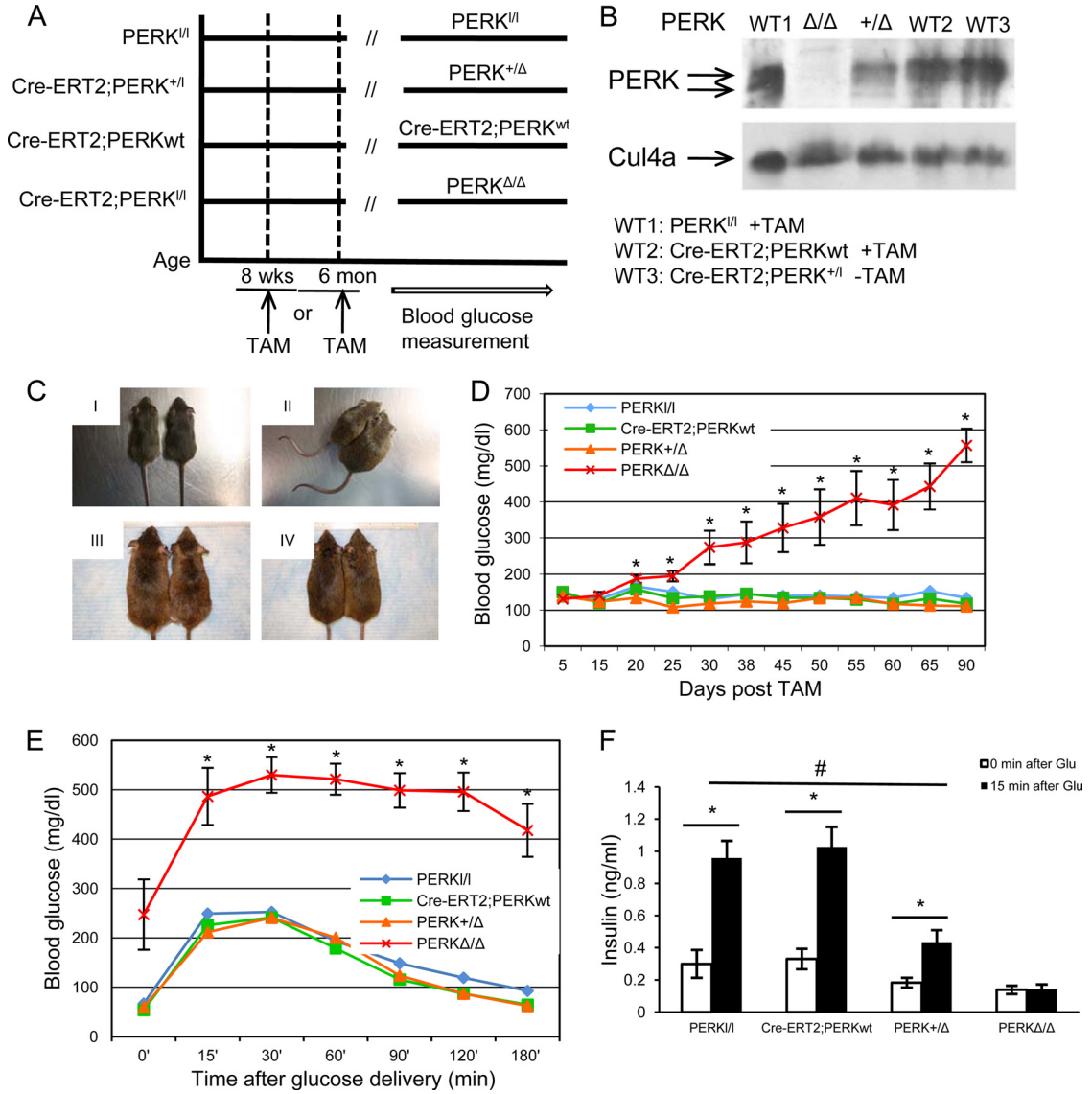


**FIG 1** Inducible PERK excision affects glucose homeostasis in adult mice. (A) Schematic representation of experimental design. At the age of 8 to 12 weeks or 6 months, Cre-ERT2; PERK$^{l/l}$ and Cre-ERT2; PERK$^{+/l}$ mice were treated with TAM by oral gavage for 5 days to generate PERK knockout (PERK$^{\Delta/\Delta}$) and heterozygous (PERK$^{+/\Delta}$) mice. PERK$^{l/l}$ and Cre-ERT2; PERKwt mice were also treated. Random-feeding blood glucose was measured every 5 or 7 days for all the cohorts. (B) Western analysis of pancreatic lysates isolated from PERK$^{\Delta/\Delta}$, PERK$^{+/\Delta}$, PERK$^{l/l}$, and Cre-ERT2; PERKwt mice 1 week after TAM treatment and Cre-ERT2; PERK$^{+/l}$ (−TAM) using anti-PERK serum. (C) Photo I, PERK$^{l/l}$ (left) and Cre-ERT2; PERK$^{l/l}$ (right) (−TAM) mice 8 weeks of age, before TAM treatment; photo II, PERK$^{\Delta/\Delta}$ (left) and PERK$^{l/l}$ (right) mice subjected to TAM-induced PERK excision at 8 weeks of age, 12 to 16 weeks post-TAM treatment; photo III, PERK$^{l/l}$ (left) and PERK$^{\Delta/\Delta}$ (right) mice; photo IV, PERK$^{l/l}$ (left) and PERK$^{+/\Delta}$ (right) mice. For photos III and IV, PERK excision was done at 6 months of age and body size was assessed at 12 to 16 weeks post-TAM treatment. (D) Blood glucose was measured every 5 days after TAM treatment ($n = 5$ to 8 mice in each case; mean ± SEM). *, $P < 0.05$. (E) Glucose tolerance test ($n = 5$ to 7 mice in each case; mean ± SEM) was performed by oral gavage at 12 weeks post-TAM treatment. *, $P < 0.05$ (PERK$^{\Delta/\Delta}$ mice versus Cre-ERT2; PERKwt, PERK$^{+/\Delta}$, and PERK$^{l/l}$ mice). (F) Blood was sampled for secreted insulin at 0 and 15 min after glucose (Glu) delivery during GTT. *, $P < 0.05$ (0 min versus 15 min); #, $P < 0.01$ (PERK$^{+/\Delta}$ mice versus Cre-ERT2; PERKwt and PERK$^{l/l}$ mice at 15 min), mean ± SEM.

insulin production and/or secretion. A significant reduction in body weight was noted at later stages following PERK loss and may reflect a role of PERK in additional secretory cell compartments besides the pancreas (see Fig. S1D) (29, 42).

**PERK excision is accompanied by pancreatic atrophy and death of insulin producing β cells.** Given the profound effect of PERK loss on glucose homeostasis, we reasoned that pancreatic dysfunction should be a contributing factor. Indeed, increasing pancreatic atrophy was noted following excision of PERK (Fig. 2C and 3B) independent of age and body size. Because acinar cells make up a majority of pancreatic mass, we infer that PERK loss triggered acinar cell loss and potentially death of endocrine cells given the profound increase in glucose levels. Indeed, hematoxylin-and-eosin-stained sections of pancreata from mice in which PERK had been excised revealed a significant reduction in islet size and integrity (Fig. 2B and 3A). We also assessed the structural integrity of individual β cells and of acinar tissue by electron microscopy. In β cells, the number of mature secretory granules was

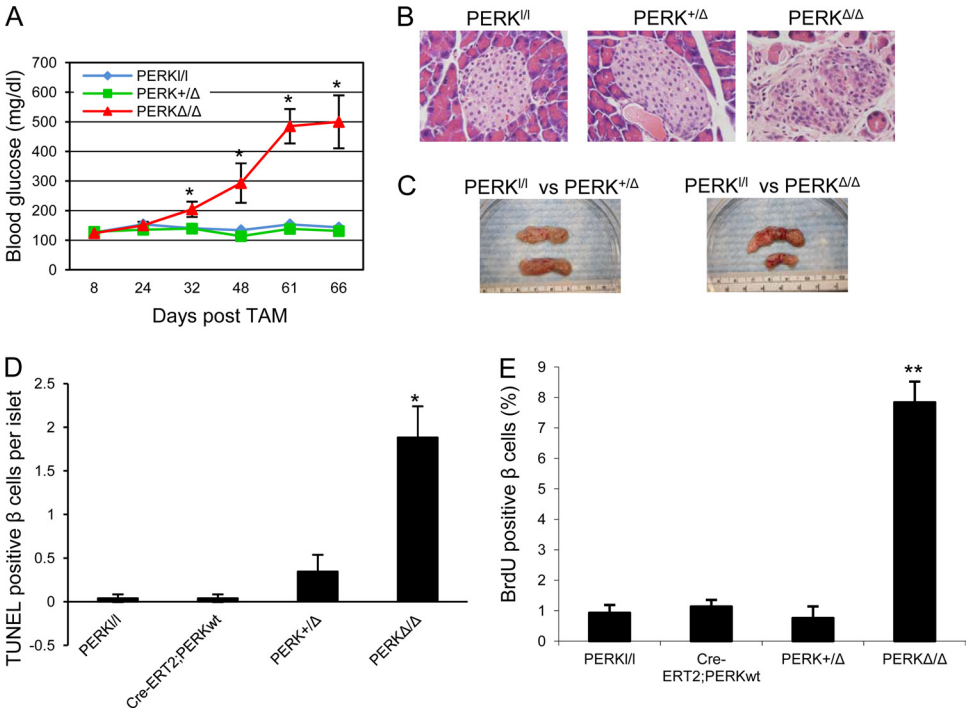


**FIG 2** PERK excision at 6 months of age triggers diabetes mellitus by 4 weeks postexcision. (A) *Perk* was acutely excised in 6-month-old mice. Blood glucose was measured regularly after the final TAM treatment, day 0 ($n = 4$ to 9 mice in each case, mean ± SEM). *, $P < 0.01$ ($PERK^{\Delta/\Delta}$ mice versus $PERK^{+/\Delta}$ and $PERK^{l/l}$ mice). (B) Mice were sacrificed 10 weeks post-TAM treatment and the whole pancreas was harvested for hematoxylin-eosin staining (40×). (C) Whole pancreata harvested from $PERK^{\Delta/\Delta}$ and control mice 16 weeks post-TAM treatment. (D) TUNEL staining in $PERK^{\Delta/\Delta}$ and control mice ($n = 4$ to 5 mice in each case, mean ± SEM). *, $P < 0.05$ ($PERK^{\Delta/\Delta}$ mice versus Cre-ERT2; PERKwt, $PERK^{+/\Delta}$, and $PERK^{l/l}$ mice). (E) Mice were continuously fed drinking water containing BrdU (1 mg/ml) for 1 week before sacrifice at 3 weeks post-TAM treatment. **, $P < 0.01$ ($n = 4$ to 5 mice in each case, mean ± SEM).

reduced and was accompanied by an increase in immature granules (Fig. 3C). Nuclei were generally distorted and compressed by membrane-bounded cisternae. The ER was grossly distended and filled with electron-dense material suggestive of abnormal retention of newly synthesized protein and consistent with accumulation of proinsulin in perinuclear structures (Fig. 4A). We also noted that the level and distribution of proinsulin in knockout β cells were distinctly different from those of the mature insulin-producing cells in wild-type islets (see Fig. S3 in the supplemental material), consistent with proinsulin accumulation resulting from impaired protein maturation and potentially a consequence of decreased translational control in the absence of PERK. Consequently, insulin mRNA level was not increased (data not shown). Acinar cells also exhibited a significant disruption of ER structure and integrity (Fig. 3C).

To address whether the onset of diabetes triggered by PERK excision is cell autonomous, we intercrossed Pdx1-CreER mice with $PERK^{l/l}$ mice to generate mice with the Pdx1-CreER; $PERK^{l/l}$ genotype (14). Critically, Pdx1 expression is restricted to pancreatic β cells in adult mice (22). Pdx1-CreER; $PERK^{l/l}$ and control mice were treated with either TAM or vehicle (Fig. 5A). We confirmed that PERK was excised only in β cells and not in the adjacent acini in β-specific $PERK^{\Delta/\Delta}$ mice (Fig. 5B). Critically, β-specific $PERK^{\Delta/\Delta}$ mice developed diabetes mellitus by 1 month post-TAM treatment (Fig. 5C). Analysis of pancreatic tissue from global PERK and β-specific $PERK^{\Delta/\Delta}$ mice revealed similar islet histologies, including reduced islet number and islet size (Fig. 5D), but without the pancreatic atrophy that occurs following global PERK excision (data not shown). This result suggests that PERK deficiency regulates β-cell homeostasis in a cell-autonomous manner.

Reduced cellularity of the pancreas could reflect increased cell death, decreased proliferation, or a combination of both. Previous reports regarding the contribution of increased β cell death versus decreased β cell proliferation to the reduction in islet size and function were based on either a conventional PERK knockout mouse model or one wherein PERK is deleted during late embryonic development (18, 43). With regard to β cell proliferation, it is important to consider that following early postnatal development, β cells are postmitotic, with fewer than 1% of the cells cycling (13, 40). With this knowledge, we reasoned that a reduction in β cell proliferation was unlikely to significantly contribute to the observed phenotype. We initially assessed β cell death using a TUNEL assay at 3 weeks post-TAM treatment (Fig. 6A, excision at 8 weeks; Fig. 2D, excision at 6 months). This time point was chosen because this is the time when blood glucose levels are only modestly elevated. At this time point we noted a significant increase in TUNEL-positive cells, consistent with elevated cell death. We also observed increased TUNEL-positive β cells in PERK-excised islets as early as 1 week post-TAM treatment (see Fig. S2A in the supplemental material), suggesting that β cell death is rapidly induced following PERK excision.

It has also been suggested that oncosis, a type of cell death characterized by cell swelling, vacuolization, chromatin fragmentation, and increased membrane permeability (31), occurs following PERK excision. We did note this morphology in PERK-defi-

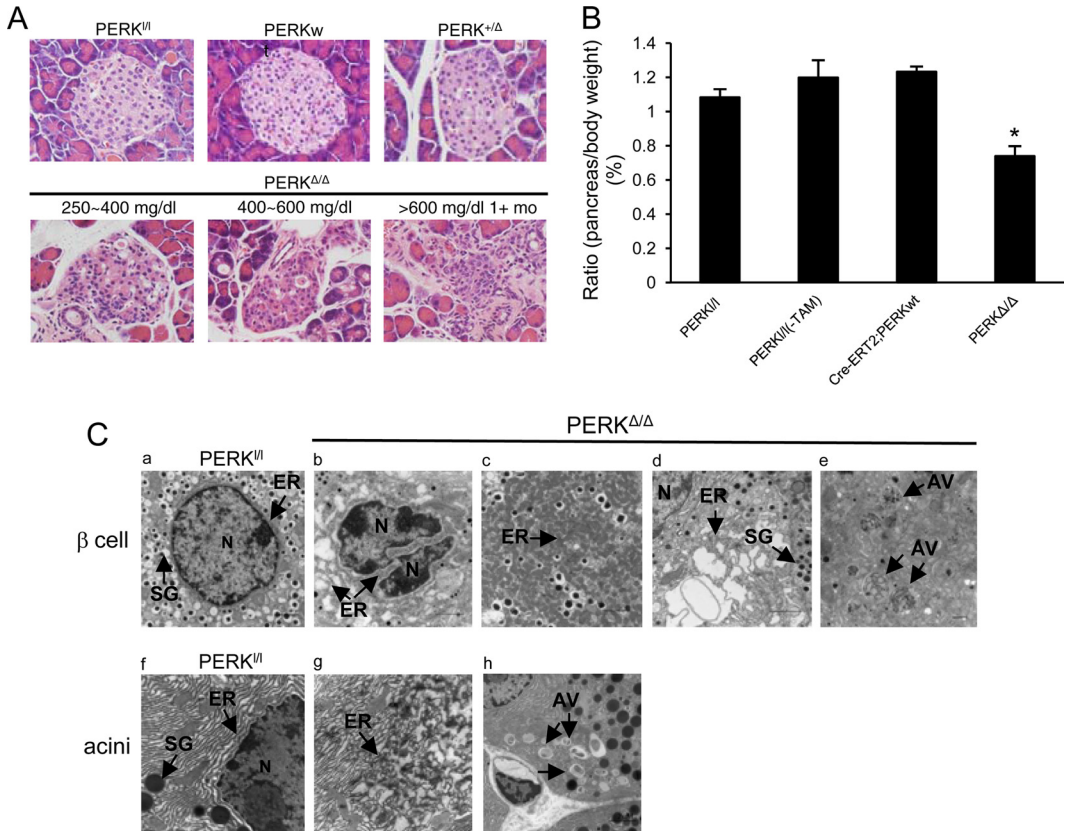


**FIG 3** PERK excision at 8 weeks of age triggers β cell death. (A) Pancreatic sections from PERK$^{\Delta/\Delta}$ and control mice 12 to 16 weeks post-TAM treatment were stained with hematoxylin-eosin (40×). (B) The whole pancreas was isolated from mice 12 to 16 weeks post-TAM treatment and weighed ($n = 4$ to 9 mice in each case; mean ± SEM). The ratio between pancreas and body weight was determined. *, $P < 0.01$ (PERK$^{\Delta/\Delta}$ mice versus Cre-ERT2; PERKwt and PERK$^{l/l}$ mice with or without TAM treatment). (C) Electron micrographs of β cells (images a to e) or acinar cells (images f to h) from PERK$^{l/l}$ and PERK$^{\Delta/\Delta}$ mice at 12 weeks post-TAM treatment. N, nuclear; ER, endoplasmic reticulum; SG, secretory granules; AV, autophagy vesicle ($n = 3$ mice in each case). The horizontal bars correspond to 500 nm.

cient β cells, although this morphology can also reflect a more general cell morphology of accumulating misfolded proteins within secretory organelles (see Fig. S2B in the supplemental material). To more directly assess the contribution of oncosis, we stained pancreata for apolipoprotein E (ApoE), a serum protein that can be passively taken up through a compromised plasma membrane during oncotic cell death (24). We did note some ApoE-positive acinar cells dispersed in the pancreata of PERK-deficient mice at 3 weeks post-TAM treatment (see Fig. S2C) but relatively few positive β cells (although the amount was statistically significant relative to that of the control) (see Fig. S2D). We conclude that apoptotic death and, to a lesser degree, oncosis contribute to decreased pancreatic cell number.

While the reduction in β cell and islet numbers is clearly a reflection of increased cell death, we were compelled to directly assess the proliferative capacity of PERK-deficient β cells given the previous evaluation of the role of proliferation during late embryonic pancreas development (43) as well as the impact of PERK deletion on the proliferative nature of tumor cells (4). Mice were continuously labeled with BrdU for 1 week starting from the prediabetic stage (2 weeks post-TAM treatment) or for 2 weeks at a frank diabetic stage. A significant increase in the percentage of proliferating β cells in all pancreata from PERK-deficient mice was noted regardless of the age at which PERK was excised (Fig. 2E and 6B and C). This result demonstrates that β cell loss is not a direct result of decreased proliferation. The increased proliferation following PERK excision may reflect PERK's established ability to regulate key cell division proteins such as cyclin D1 and thereby prevent inappropriate proliferation (6, 16). To test this hypothesis, we assessed cyclin D1 expression by immunofluorescence and by immunoblotting using purified islets. Cyclin D1 expression was elevated significantly in PERK-excised β cells (Fig. 6D); importantly, assessment was made in mice with only modestly elevated glucose rather than late-stage diabetic mice to eliminate confounding effects of high glucose levels on cyclin D1 expression (11, 12). A robust increase in cyclin D1 accumulation was also noted by immunoblotting; this increase was accompanied by a coordinate increase in phosphorylated Rb consistent with increased, functionally active cyclin D1-dependent kinase complexes (Fig. 7A, right).

**PERK excision results in ER malfunction and activation of UPR signaling.** Since PERK excision resulted in the rapid and dramatic impairment of β cell function and survival, we reasoned that PERK loss should compromise protein quality control in the ER, resulting in the accumulation of misfolded proteins, with misfolded insulin, proinsulin, and glucose transporters (e.g., Glut2) being of particular significance. Consistent with this supposition, we noted accumulation of Glut2 in perinuclear regions in

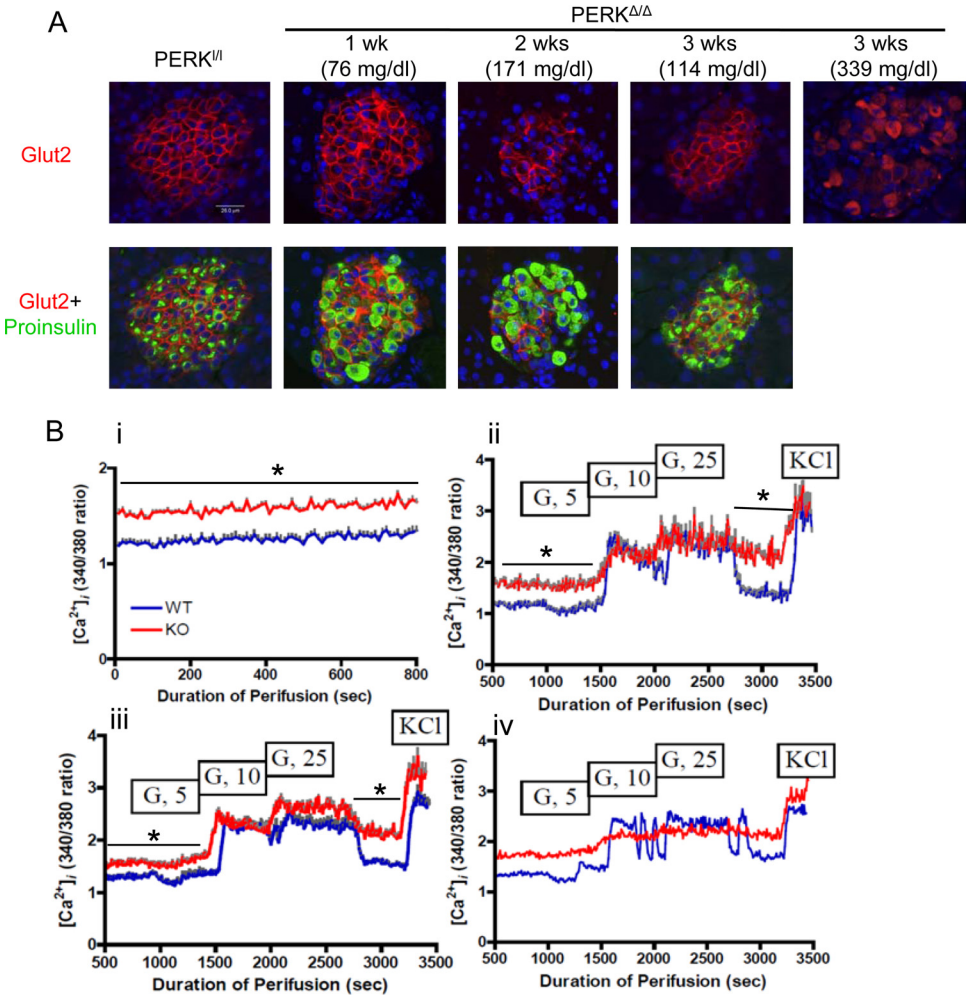


**FIG 4** PERK excision in 8-week-old mice triggers anomalous accumulation of proinsulin and Glut2 in β cell ER. (A) The top row shows representative immunofluorescent staining of Glut2 (red) in PERK$^{l/l}$ or PERK$^{\Delta/\Delta}$ β cells 3 weeks post-TAM treatment; the bottom row provides representative immunofluorescent staining for proinsulin (green) and Glut2 (red) in β cells. (B) Cytosolic calcium was measured in islets isolated from PERK$^{l/l}$ (blue) and PERK$^{\Delta/\Delta}$ (red) mice at 1 week (i and ii), 2 weeks (iii), or 3 to 5 weeks (iv) post-TAM treatment. Primary islets were isolated from 1 or 2 mice of each genotype, and 12 random islets from each genotype were selected for this experiment. Basal $[Ca^{2+}]_i$ level and response to stepwise stimulation by glucose (G; 5, 10, and 25 mM) were observed. The colored solid line represents the mean, and the vertical gray line represents the SEM. *, $P < 0.01$ (PERK$^{\Delta/\Delta}$ mice versus PERK$^{l/l}$ mice).

PERK$^{\Delta/\Delta}$ islets by 3 weeks and proinsulin by 1 week post-PERK excision (Fig. 4A). The noted inappropriate accumulation occurred prior to the gross abnormalities in blood glucose levels, suggesting that ER malfunction occurred in early, prediabetic cells. The ER accumulation of glucose transporters was not observed in the liver or peripheral tissues such as adipose or muscle tissue (see Fig. S4A, B, and C in the supplemental material). In addition, we detected no obvious pathological changes in the salivary glands of PERK knockout mice (see Fig. S4D), highlighting the importance of PERK function within the pancreatic islet. Although blood glucose levels were only slightly elevated at this time, purified islets from PERK$^{\Delta/\Delta}$ mice did not exhibit a statistically significant reduction in glucose-stimulated insulin secretion (GSIS) with gradually increasing glucose concentrations (glucose ramp) with normal basal insulin secretion (see Fig. S5A in the supplemental material), demonstrating that insulin secretion is compromised at this early time point. These results are suggestive of a general defect in protein maturation in the ER.

The ATP-sensitive $K^+$ ($K_{ATP}$) channels play a critical role in coupling membrane excitability to GSIS to maintain blood glucose within a narrow physiological range in islet β cells. Increased glucose metabolism results in elevated intracellular [ATP]:[ADP], closure of $K_{ATP}$ channels, and membrane depolarization, thereby inducing voltage-dependent $Ca^{2+}$ entry, which then triggers insulin secretion. Conversely, a decrease in metabolic signals opens $K_{ATP}$ channels and suppresses the electrical trigger of insulin secretion (25, 33). To determine whether a protein maturation defect extends to $K_{ATP}$ channels, we assessed $K_{ATP}$ functionality by employing glyburide (an antagonist of $K_{ATP}$ channels) to effectively inhibit $K_{ATP}$ channel activity on the β cell membrane, prior to assessing insulin release. As shown in Fig. S5B and C in the supplemental material, no significant difference in insulin release was observed in PERK-excised islets relative to control islets challenged with either the glyburide ramp or maximal depolarization of the cytoplasm membrane (KCl, 30 mM).

The ER is a major cellular calcium storage organelle, and ER

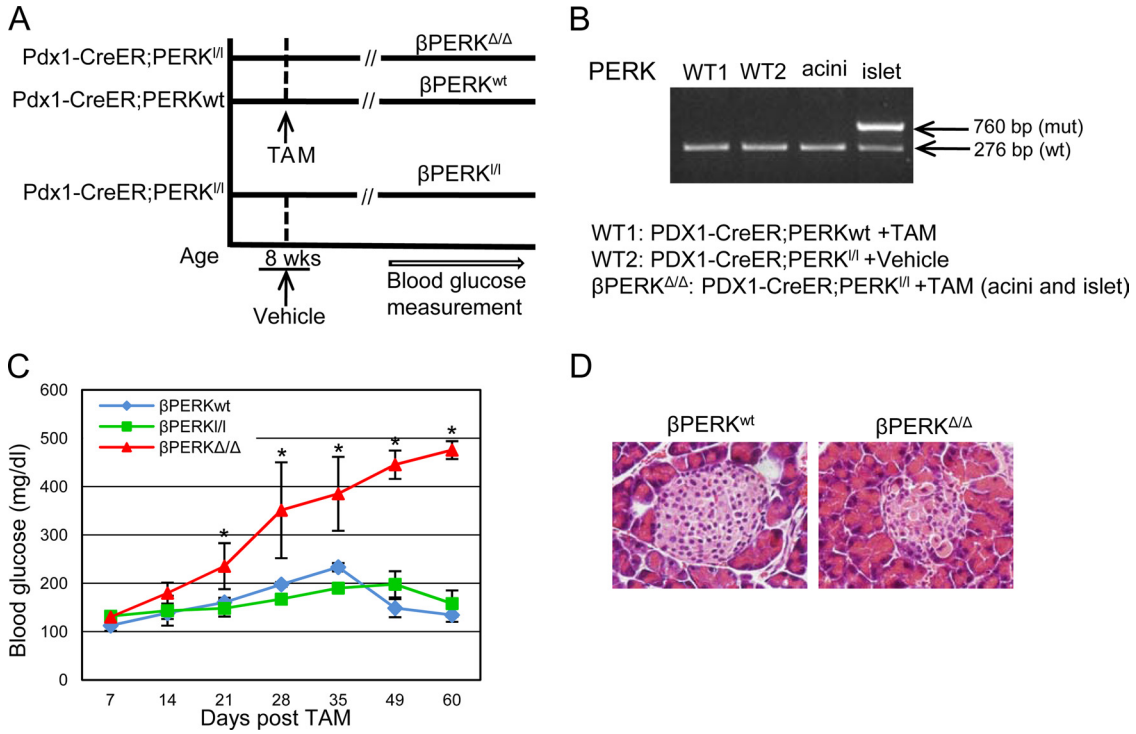


**FIG 5** β cell-specific PERK knockout in young adult mice triggers rapid onset of hyperglycemia. (A) Schematic of experimental design. (B) Pdx1-Cre mice were treated with TAM at 8 weeks of age. PERK excision PCR was performed on primary islets or acini isolated 5 days post-TAM treatment. (C) Time course of blood glucose concentration ($n = 4$ to 8 mice in each case, mean ± SEM; $P < 0.01$). (D) All mice were sacrificed 9 weeks post-TAM treatment and the whole pancreas was analyzed. Pancreatic sections were stained with hematoxylin-eosin and photographs were taken (40×).

calcium homeostasis is critical for protein folding and processing (35). Low glucose concentrations lead to a concentration-dependent reduction in $[Ca^{2+}]_{ER}$ that parallels an increase in PERK activation (32), implicating PERK as a potential $Ca^{2+}$ sensor in the ER. However, there is no clear evidence to show when and how $Ca^{2+}$ signals behave abnormally after PERK acute loss in islets. We monitored $[Ca^{2+}]_i$ regulation in purified islets at 1, 2, and 3 to 5 weeks (a point where blood glucose was >300 mg/dl) after PERK excision. While basal $[Ca^{2+}]_i$ was elevated (Fig. 4B, graph i), $Ca^{2+}$ oscillation in response to serial glucose concentrations (5, 10, and 25 mM) in PERK-excised islets was decreased (Fig. 4B, graphs ii to iv), supporting a disturbance in $[Ca^{2+}]_i$ homeostasis in prediabetic PERK-deficient islets.

**Activation of Ire and ATF6 signaling in PERK-excised islets.** Loss of PERK is expected to deregulate protein flux through the ER, contributing to increased protein misfolding, which should, in turn, increase ER stress, resulting in increased flux through the remaining intact UPR signaling pathways. We interrogated the activation status of Ire1 and ATF6 by immunoblotting lysates generated from purified islets generated from PERK knockout and control mice at a prediabetic stage (1 or 2 weeks postexcision). Consistent with deletion of PERK, we did not observe increased p-eIF2α in PERK-excised islets (Fig. 7A). In contrast, we noted a significant increase in BiP (both mRNA and protein levels), Ire1, and p-JNK, whose activation is dependent on Ire1 (Fig. 7A, top, and B) (23). We also observed increased accumulation of spliced Xbp1 (sXBP1) protein (Fig. 7A, bottom), consistent with increased Ire1 activity. Grp94 mRNA levels were also significantly increased (Fig. 7B). Moreover, PERK excision was accompanied by increased accumulation of cleaved ATF6 (Fig. 7A, bottom). As expected, the mRNA levels of *chop*, *Der-1*, and *EDEM*, the last two being PERK-regulated components of the ER-associated protein degradation (ERAD) pathway, were not significantly changed (41).

The data provided reveal significant distention of β cell ER (Fig. 3C), likely a reflection of accumulation of misfolded proteins (e.g., proinsulin and Glut2 [Fig. 4A]), ultimately triggering activation of the remaining branches of the UPR and cell death. We reasoned that if the demand for endogenous production of insulin in the mature islet could be reduced, then ER stress and proteotoxicity should be decreased in PERK-excised islets and thereby reduce β cell death. To test this, exogenous insulin was administered, at the time of PERK excision, to reduce the need for increased insulin synthesis and secretion. At 3 weeks post-PERK deletion, a point where loss of islet integrity routinely becomes apparent histologically along with increased β cell death, a significant increase in β cell death was again noted in PERK-excised islets. However, insulin treatment decreased the fraction of TUNEL-positive β cells relative to that obtained with vehicle treatment (Fig. 7C). These results demonstrate that a treatment that reduces protein load in the ER (e.g., insulin) of β cells reduces cell death, consistent with protein misfolding functioning as the cell death trigger.

## DISCUSSION

PERK is a key regulator of protein translation, particularly at points where the functional capacity of the secretory apparatus of cells is overwhelmed by protein influx. During these periods,

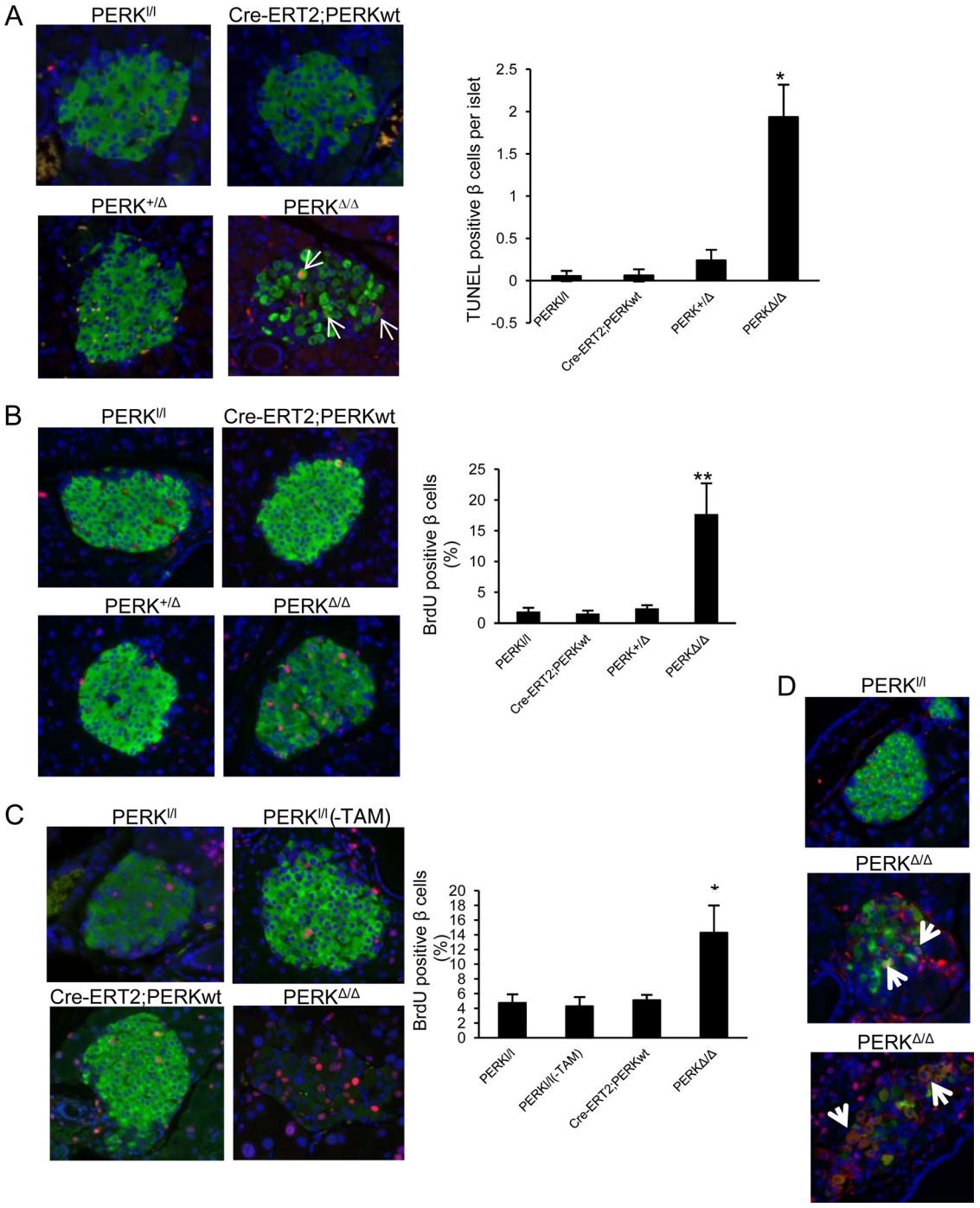


**FIG 6** PERK excision at 8 weeks of age induces β cell apoptosis and proliferation. (A) β cell death was assessed by TUNEL at 3 weeks post-TAM treatment. Arrows indicate TUNEL (red), insulin (green), and DAPI triple positive cells. The graph represents quantification of TUNEL-positive and insulin-positive cells ($n$ = 4 to 6 mice in each case; mean ± SEM). *, $P < 0.01$ ($PERK^{\Delta/\Delta}$ mice versus Cre-ERT2; PERKwt, $PERK^{+/\Delta}$, and $PERK^{l/l}$ mice). (B and C) Mice were continuously fed with BrdU in drinking water for 1 week right before and sacrificed at 3 weeks after TAM treatment (B) ($n$ = 5 mice in each case; mean ± SEM) or 2 weeks before and sacrificed at 12 weeks after TAM treatment (C) ($n$ = 3 to 6 mice in each case; mean ± SEM). **, $P < 0.01$ ($PERK^{\Delta/\Delta}$ mice versus Cre-ERT2; PERKwt, $PERK^{+/\Delta}$, and $PERK^{l/l}$ mice). *, $P < 0.05$ ($PERK^{\Delta/\Delta}$ mice versus Cre-ERT2; PERKwt and $PERK^{l/l}$ mice with or without TAM treatment). Green, insulin; red, BrdU. (D) Paraffin-embedded pancreas sections from mice at 3 weeks post-TAM treatment were immunostained with anti-cyclin D1 antibody. Arrows indicate cyclin D1, insulin, and DAPI triple positive cells or cyclin D1 and insulin double positive cells. Green, insulin; red, cyclin D1.

PERK-dependent inhibition of protein translation and cell cycle progression provides a window of opportunity for cells to re-equilibrate and thereby prevent irreparable damage (7, 20). PERK-deficient cells are particularly sensitive *in vitro* to exogenous stresses that compromise ER folding capacity (10). *In vivo*, conventional PERK knockout mice develop neonatal diabetes and exhibit phenotypes consistent with compromised protein maturation in secretory tissues during postnatal development (18, 42,

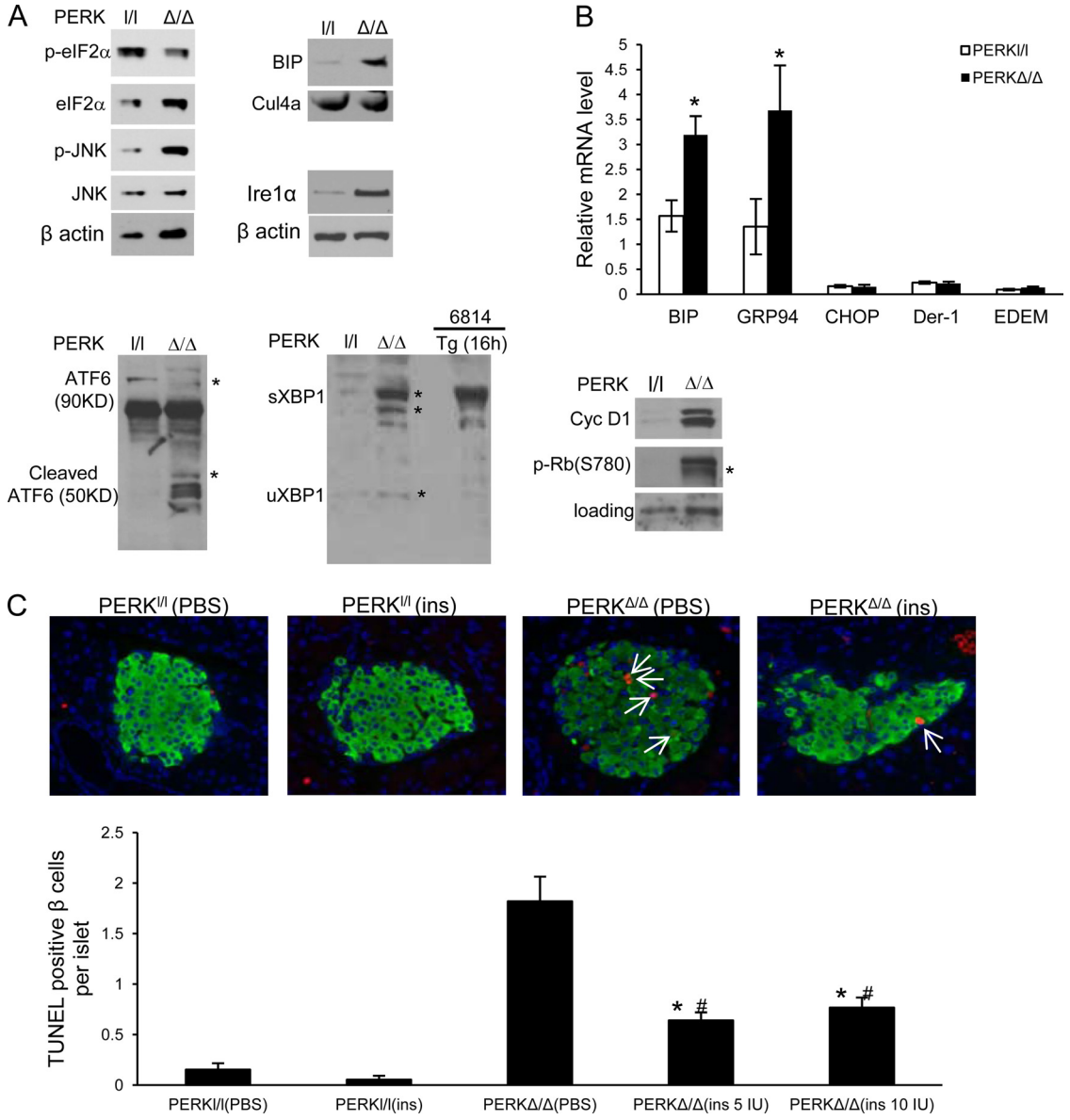


**FIG 7** Activation of Ire and ATF6 in PERK knockout islets at 8 weeks of age. Primary islets were isolated from PERK$^{l/l}$ and PERK$^{\Delta/\Delta}$ mice 1 to 2 weeks after tamoxifen treatment. Western blotting (A) or qPCR ($n = 9$, mean ± SEM) (B) was performed to assess activation of Ire and ATF6 or their downstream effectors as indicated. T cell lymphoma 6814 was treated with thapsigargin for 16 h and served as a positive control. ATF6, sXBP1, and cyclin D1 blots use the same loading control. *, $P < 0.05$ (PERK$^{\Delta/\Delta}$ mice versus PERK$^{l/l}$ mice). (C) β cell death was assessed by TUNEL at 3 weeks post-TAM treatment. Mice received insulin (5 IU/kg or 10 IU/kg) or PBS once daily from onset of TAM administration. Green, insulin; red, TUNEL. Arrows indicate TUNEL, insulin (ins), and DAPI triple positive cells. The graph represents quantification of TUNEL-positive and insulin-positive cells ($n = 4$ to 6, mean ± SEM). *, $P < 0.01$ (PERK$^{\Delta/\Delta}$ mice [ins, 5 IU/kg or 10 IU/kg] versus PERK$^{\Delta/\Delta}$ mice [PBS]). #, $P < 0.01$ (PERK$^{\Delta/\Delta}$ mice [ins, 5 IU/kg or 10 IU/kg] versus PERK$^{l/l}$ mice [PBS or ins]).

43). Consistent with a requisite role for PERK in maintaining pancreatic and glucose homeostasis, mice that harbor nonphosphorylatable eIF2α alleles (eIF2αS51A) also exhibit severe defects in pancreatic function and glucose homeostasis (36).

It should be noted that the pancreatic phenotype previously described was suggested to reflect a unique role for PERK from the late embryo (embryonic day 13.5) to early postnatal (postnatal day 4) stage (43). However, it remained plausible that this conclusion reflects employment of an approach which utilized late embryonic deletion of PERK driven by a developmentally regulated Cre allele, resulting in a slow decline in PERK levels which ultimately favored compensatory action by the remaining eIF2α kinases, as has been observed in cultured cells (16). To directly address the role of PERK in adult tissue, we used a tamoxifen-inducible Cre allele driven by a ubiquitous promoter to excise *perk* in young adult and fully mature mice. Because of recent interest in targeting PERK as a mechanism to antagonize neoplastic growth (2–4), we utilized this genetic approach to interrogate PERK function in adult tissue, as it approximates what might be achieved using small-molecule inhibitors of PERK. Regardless of the age at which PERK was excised, rapid and profound pancreatic atrophy was observed; this was paralleled by a specific loss of both insulin-producing β cells and exocrine acinar tissue. This was accompanied by the onset of hyperglycemia within 3 to 4 weeks of PERK

deletion. Regular monitoring of blood glucose in mice maintained on normal chow revealed blood glucose levels increasing significantly by 3 weeks post-PERK excision and ultimately reaching levels above 600 mg/dl 8 weeks postexcision. As would be expected, mice were glucose intolerant and exhibited low levels of circulating insulin, suggesting a defect in insulin production; mice still remained responsive to exogenous insulin.

Since PERK regulates protein synthesis and thus protein load in the ER, we anticipated that reduced insulin content might result from luminal accumulation of proinsulin, a result of a failure to process newly synthesized protein. Consistent with this notion, we noted increased perinuclear accumulation of proinsulin and Glut2. Electron microscopic analysis revealed distorted and engorged ER structures frequently containing electron-dense material. Strikingly, the reduced membrane targeting of glucose transporters was specific to β cells, as no such alteration was noted in multiple other tissues. In addition, we failed to note aberration in other secretory tissues such as the salivary gland (see Fig. S4D in the supplemental material) and mammary tissue (5). Collectively, these observations suggest that in the absence of PERK, protein maturation in the ER of β cells is significantly compromised.

Although β cells are weakly proliferative in mice by 8 weeks of age, we noted that PERK excision was accompanied by a significant increase in β cell proliferation. This is in contrast to the phenotype of mice in which deletion of PERK during late embryonic development appears to result in reduced proliferation (43). The noted increase in proliferation occurs coordinately with overexpression of cyclin D1, a regulator of cell cycle reentry and $G_1$ progression (6, 16, 38), likely a feature of increased cyclin D1 translation, which has previously been observed in PERK-deficient cells (16). Indeed, increased cyclin D-dependent kinase activity in β cells is sufficient to increase proliferation (11, 39). Alternatively, the increase in proliferation could also reflect increased levels of glucose, which acts as a potent β cell mitogen. While these mechanisms are not mutually exclusive, increased proliferation is noted at time points where glucose levels are only marginally elevated, suggesting that the primary cause pertains to reduced PERK-dependent translational inhibition of cyclin D1 and the secondary cause is a glucose-dependent mitogenic effect.

With the dramatic increase in proliferation, what is the underlying cause of β cell and islet loss? PERK excision was accompanied by a distinct and significant increase in β cell death. This would suggest that increased proliferation is not sufficient to maintain β cell mass. In fact, inappropriate S-phase entry, which can be triggered by cyclin D1, can contribute to apoptosis (17). However, it is important to consider that in the context of β cells, previous work suggests that increased cyclin D1- or D2-dependent catalytic activity can increase β cell proliferation without compromising survival (21, 39). Indeed, a more likely cell death trigger is the accumulation of misfolded proteins in the ER due to loss of translational control by PERK. The ensuing ER stress would then trigger activation of other branches of the UPR such as Ire1 and ATF6 as well as their downstream targets Xbp1 and JNK (23), resulting in activation of proapoptotic signaling pathway. While oxidative stress is implicated in β cell damage and death both in eIF2αS51A homozygous mice (1) and in tissue-specific PERK knockout models (4), we failed to detect increased reactive oxygen species (ROS) accumulation in PERK-deficient islets, which should accompany oxidative stress.

What is the relative importance of β cell death versus β cell dysfunction? PERK excision at 1 week post-TAM treatment has little effect on insulin release stimulated either by glucose or by glyburide in isolated primary islets. However, the basal $[Ca^{2+}]_i$ in PERK-excised islets does increase significantly, and this is accompanied by increased proapoptotic phospho-JNK signaling, which could potentially affect β cell metabolism and survival. Indeed, we noted increased apoptotic β cell death 1 week post-PERK excision, suggesting that a fraction of β cells die at this very early stage after PERK loss. Thus, β cell death rapidly ensues upon PERK loss and progressively increases concurrent with increased accumulation of proinsulin.

In the current study, we introduced an acute PERK deletion system which, unlike other approaches, allowed us to assess PERK function in mature islets postdevelopment. The results provided demonstrate that in contrast to previous predictions (43), loss of PERK function triggers the rapid onset of insulin-dependent diabetes regardless of age. An important remaining issue is whether PERK is a viable target for anticancer therapy. Ample evidence supports a role for PERK in the facilitation of tumor progression and tumor metastasis (4, 26, 30). Tumors generally utilize intrinsic survival pathways to maintain homeostasis under suboptimal growth conditions and thereby prevent cell death; an addiction to these prosurvival pathways has been referred to as "nononcogene addiction," and such pathways are now considered potential therapeutic targets for cancer. If PERK does not play a requisite role in adult tissue homeostasis but is required for tumor cell growth and survival, generation of small-molecule regulators of PERK would be highly attractive. However, our results suggest that while use of small-molecule PERK inhibitors may have significant antineoplastic activity, PERK inhibition will also be associated with islet dysfunction and onset of insulin-dependent diabetes. However, our data also suggest that insulin supplementation may reduce protein load and offset β cell death and thereby prevent diabetes occurrence. Additional work is required to discern the feasibility of such approaches.

## ACKNOWLEDGMENTS

We thank Margarita Romero for outstanding technical assistance, Douglas R. Cavener (Pennsylvania State University) for providing $PERK^{loxP/loxP}$ mice, Eric J. Brown (University of Pennsylvania) for providing CRE-ERT2 mice, Xianxin Hua (University of Pennsylvania) for providing PDX-Cre mice, and the AFCRI histology core.

This work was supported by National Institutes of Health grants P01 CA104838 (M.C.S. and J.A.D.) and a Leukemia & Lymphoma Scholar award (J.A.D.).

## REFERENCES

1. **Back SH, et al.** 2009. Translation attenuation through eIF2alpha phosphorylation prevents oxidative stress and maintains the differentiated state in beta cells. Cell Metab. **10**:13–26.
2. **Bi M, et al.** 2005. ER stress-regulated translation increases tolerance to extreme hypoxia and promotes tumor growth. EMBO J. **24**:3470–3481.
3. **Blais JD, et al.** 2006. Perk-dependent translational regulation promotes tumor cell adaptation and angiogenesis in response to hypoxic stress. Mol. Cell. Biol. **26**:9517–9532.
4. **Bobrovnikova-Marjon E, et al.** 2010. PERK promotes cancer cell proliferation and tumor growth by limiting oxidative DNA damage. Oncogene **29**:3881–3895.
5. **Bobrovnikova-Marjon E, et al.** 2008. PERK-dependent regulation of lipogenesis during mouse mammary gland development and adipocyte differentiation. Proc. Natl. Acad. Sci. U. S. A. **105**:16314–16319.
6. **Brewer JW, Diehl JA.** 2000. PERK mediates cell-cycle exit during the mammalian unfolded protein response. Proc. Natl. Acad. Sci. U. S. A. **97**:12625–12630.

7. **Brewer JW, Hendershot LM, Sherr CJ, Diehl JA.** 1999. Mammalian unfolded protein response inhibits cyclin D1 translation and cell-cycle progression. Proc. Natl. Acad. Sci. U. S. A. **96**:8505–8510.
8. **Cavener DR, Gupta S, McGrath BC.** 2010. PERK in beta cell biology and insulin biogenesis. Trends Endocrinol. Metab. **21**:714–721.
9. **Diehl JA, Fuchs SY, Koumenis C.** 2011. The cell biology of the unfolded protein response. Gastroenterology **141**:38–41.e2.
10. **Feng D, Wei J, Gupta S, McGrath BC, Cavener DR.** 2009. Acute ablation of PERK results in ER dysfunctions followed by reduced insulin secretion and cell proliferation. BMC Cell Biol. **10**:61.
11. **Fiaschi-Taesch N, et al.** 2009. Survey of the human pancreatic beta-cell G1/S proteome reveals a potential therapeutic role for cdk-6 and cyclin D1 in enhancing human beta-cell replication and function in vivo. Diabetes **58**:882–893.
12. **Fiaschi-Taesch NM, et al.** 2010. Induction of human beta-cell proliferation and engraftment using a single G1/S regulatory molecule, cdk6. Diabetes **59**:1926–1936.
13. **Finegood DT, Scaglia L, Bonner-Weir S.** 1995. Dynamics of beta-cell mass in the growing rat pancreas. Estimation with a simple mathematical model. Diabetes **44**:249–256.
14. **Gu G, Dubauskaite J, Melton DA.** 2002. Direct evidence for the pancreatic lineage: NGN3+ cells are islet progenitors and are distinct from duct progenitors. Development **129**:2447–2457.
15. **Halban PA.** 1991. Structural domains and molecular lifestyles of insulin and its precursors in the pancreatic beta cell. Diabetologia **34**:767–778.
16. **Hamanaka RB, Bennett BS, Cullinan SB, Diehl JA.** 2005. PERK and GCN2 contribute to eIF2alpha phosphorylation and cell cycle arrest after activation of the unfolded protein response pathway. Mol. Biol. Cell **16**: 5493–5501.
17. **Han EK, et al.** 1996. Increased expression of cyclin D1 in a murine mammary epithelial cell line induces p27kip1, inhibits growth, and enhances apoptosis. Cell Growth Differ. **7**:699–710.
18. **Harding HP, et al.** 2001. Diabetes mellitus and exocrine pancreatic dysfunction in perk−/− mice reveals a role for translational control in secretory cell survival. Mol. Cell **7**:1153–1163.
19. **Harding HP, Zhang Y, Bertolotti A, Zeng H, Ron D.** 2000. Perk is essential for translational regulation and cell survival during the unfolded protein response. Mol. Cell **5**:897–904.
20. **Harding HP, Zhang Y, Ron D.** 1999. Protein translation and folding are coupled by an endoplasmic-reticulum-resident kinase. Nature **397**:271–274.
21. **He LM, et al.** 2009. Cyclin D2 protein stability is regulated in pancreatic beta-cells. Mol. Endocrinol. **23**:1865–1875.
22. **Holland AM, Gonez LJ, Naselli G, Macdonald RJ, Harrison LC.** 2005. Conditional expression demonstrates the role of the homeodomain transcription factor Pdx1 in maintenance and regeneration of beta-cells in the adult pancreas. Diabetes **54**:2586–2595.
23. **Hotamisligil GS.** 2010. Endoplasmic reticulum stress and the inflammatory basis of metabolic disease. Cell **140**:900–917.
24. **Iida K, Li Y, McGrath BC, Frank A, Cavener DR.** 2007. PERK eIF2 alpha kinase is required to regulate the viability of the exocrine pancreas in mice. BMC Cell Biol. **8**:38.
25. **Koster JC, Marshall BA, Ensor N, Corbett JA, Nichols CG.** 2000. Targeted overactivity of beta cell K(ATP) channels induces profound neonatal diabetes. Cell **100**:645–654.
26. **Koumenis C.** 2006. ER stress, hypoxia tolerance and tumor progression. Curr. Mol. Med. **6**:55–69.
27. **Li C, et al.** 2010. Mechanism of hyperinsulinism in short-chain 3-hydroxyacyl-CoA dehydrogenase deficiency involves activation of glutamate dehydrogenase. J. Biol. Chem. **285**:31806–31818.
28. **Li C, et al.** 2006. Effects of a GTP-insensitive mutation of glutamate dehydrogenase on insulin secretion in transgenic mice. J. Biol. Chem. **281**:15064–15072.
29. **Li Y, et al.** 2003. PERK eIF2alpha kinase regulates neonatal growth by controlling the expression of circulating insulin-like growth factor-I derived from the liver. Endocrinology **144**:3505–3513.
30. **Luo B, Lee AS.** 16 April 2012. The critical roles of endoplasmic reticulum chaperones and unfolded protein response in tumorigenesis and anticancer therapies. Oncogene. doi:10.1038/onc.2012.130. [Epub ahead of print.
31. **Majno G, Joris I.** 1995. Apoptosis, oncosis, and necrosis. An overview of cell death. Am. J. Pathol. **146**:3–15.
32. **Moore CE, Omikorede O, Gomez E, Willars GB, Herbert TP.** 2011. PERK activation at low glucose concentration is mediated by SERCA pump inhibition and confers preemptive cytoprotection to pancreatic beta-cells. Mol. Endocrinol. **25**:315–326.
33. **Remedi MS, et al.** 2009. Secondary consequences of beta cell inexcitability: identification and prevention in a murine model of K(ATP)-induced neonatal diabetes mellitus. Cell Metab. **9**:140–151.
34. **Ruzankina Y, et al.** 2007. Deletion of the developmentally essential gene ATR in adult mice leads to age-related phenotypes and stem cell loss. Cell Stem Cell **1**:113–126.
35. **Sambrook JF.** 1990. The involvement of calcium in transport of secretory proteins from the endoplasmic reticulum. Cell **61**:197–199.
36. **Scheuner D, et al.** 2001. Translational control is required for the unfolded protein response and in vivo glucose homeostasis. Mol. Cell **7**:1165–1176.
37. **Senée V, et al.** 2004. Wolcott-Rallison syndrome: clinical, genetic, and functional study of EIF2AK3 mutations and suggestion of genetic heterogeneity. Diabetes **53**:1876–1883.
38. **Sherr CJ.** 1994. G1 phase progression: cycling on cue. Cell **79**:551–555.
39. **Takane KK, Kleinberger JW, Salim FG, Fiaschi-Taesch NM, Stewart AF.** 2012. Regulated and reversible induction of adult human beta-cell replication. Diabetes **61**:418–424.
40. **Teta M, Long SY, Wartschow LM, Rankin MM, Kushner JA.** 2005. Very slow turnover of beta-cells in aged adult mice. Diabetes **54**:2557–2567.
41. **Tsai YC, Weissman AM.** 2010. The unfolded protein response, degradation from endoplasmic reticulum, and cancer. Genes Cancer **1**:764–778.
42. **Zhang P, et al.** 2002. The PERK eukaryotic initiation factor 2 alpha kinase is required for the development of the skeletal system, postnatal growth, and the function and viability of the pancreas. Mol. Cell. Biol. **22**:3864–3874.
43. **Zhang W, et al.** 2006. PERK EIF2AK3 control of pancreatic beta cell differentiation and proliferation is required for postnatal glucose homeostasis. Cell Metab. **4**:491–497.